Transcriptomic analysis of brain tissues identifies a role for CCAAT enhancer binding protein β in HIV-associated neurocognitive disorders

Saranya Canchi
University of California San Diego
Mary K. Swinton
University of California San Diego
Robert A. Rissman
University of California San Diego
Jerel Adam Fields (jafields@ucsd.edu)
University of California San Diego https://orcid.org/0000-0002-8168-1412

Research

Keywords: HIV, C/EBPβ, neuron, astroglia, neuroinflammation, transcriptomics

Posted Date: November 14th, 2019

DOI: https://doi.org/10.21203/rs.2.17235/v1

Version of Record: A version of this preprint was published at Journal of Neuroinflammation on April 11th, 2020. See the published version at https://doi.org/10.1186/s12974-020-01781-w.

Abstract

HIV-associated neurocognitive disorders (HAND) persist in the era of combined antiretroviral therapy (ART) despite reductions in viral load (VL) and overall disease severity. The mechanisms underlying HAND in ART era are not well understood but are likely multifactorial, involving alterations in common pathways such as inflammation, autophagy, neurogenesis, and mitochondrial function. Newly developed omics approaches hold potential to identify mechanisms driving neuropathogenesis of HIV in the ART era. Methods: In this study, using 33 postmortem frontal cortex (FC) tissues, neuropathological, molecular, and biochemical analyses were used to determine cellular localization and validate expression levels of the prolific transcription factor (TF), CCAAT enhancer binding protein (C/EBP) β, in brain tissues from HIV+ cognitively normal and HAND cases. Transcriptomics analyses were performed on frontal cortex tissues 24 of the FC specimens from well-characterized people with HIV that had undergone neurocognitive assessments. In vitro models for brain cells were used to investigate the role of C/EBPβ in mediating gene expression. Results:The most robust signal for TF dysregulation was observed in cases diagnosed with Minor Neurocognitive Disorders (MND) compared to cognitive normal (CN) cases. Of particular interest, due to its role in inflammation, autophagy and neurogenesis, C/EBPβ was significantly upregulated in MND compared to CN brains. C/EBPβ was increased at the protein level in HAND brains. C/EBPβ levels were significantly reduced in neurons and increased in astroglia in HAND brains compared to CN. Transfection of human astroglial cells with a plasmid (p) expressing C/EBPβ induced mRNA expression of multiple targets identified in the transcriptomic analysis of HAND brains, including dynamin-1-like protein and interleukin-1 receptor-associated kinase 1. Conclusions:These findings are the first to present transcriptomic analyses of HIV+ brain tissues, providing further evidence of altered neuroinflammation, neurogenesis, mitochondrial function, and autophagy in HAND. Interestingly, these studies confirm a role for CEBPβ in regulating inflammation, metabolism, and autophagy in astroglia. Therapeutic strategies aimed at transcriptional regulation of astroglia or downstream pathways may provide relief to HIV+ patients at risk for HAND and other neurological disorders.

Background

The number of human immunodeficiency virus (HIV) cases has increased to over 34 million individuals worldwide and neurological disorders remain prevalent despite the advent of combined antiretroviral therapies (ART). While ART has increased the life expectancy of people with HIV (PWH), HIV-associated neurocognitive disorders (HAND) have become more prevalent or remained at the same levels (Bingham *et al*, 2011; Clifford and Ances, 2013). HAND severity varies from deficiencies that do not affect daily living, asymptomatic neurocognitive impairment (ANI), to more severe neurocognitive diagnoses such as minor neurocognitive dysfunction (MND) and in rare cases HIV Associated Dementia (HAD) (Tozzi, 2003). The identification of novel mechanisms underlying HAND are needed to develop therapeutic strategies for PWH.

Multiple pathogenic mechanisms are implicated as contributing to HAND progression and they may stem from ART-induced neurotoxicity, HIV protein interactions with uninfected bystander cells, low-level viral replication, and neuroinflammation(Fields *et al*, 2015b; Nath, 2002). Untargeted transcriptomics analyses offer the promise of uncovering novel mechanisms that are relevant to HAND in the era of ART. These mechanisms may be missed by more traditional approaches that focus on specific pathways or biomarkers of interest. Characterizing alterations in the transcriptome in brains of HAND cases compared to HIV+ cognitive normal cases could lead to the discover of important factors or pathways for the development of therapeutic strategies.

Transcription factors (TF) can contribute to health and disease by regulating the expression genes involved important pathways. For example, TFs have been implicated in altering function of pathways such as mitochondrial biogenesis, autophagy and inflammation in multiple neurodegenerative diseases including Alzheimer's disease, Parkinson's disease, and HAND. TFs make for promising therapeutic targets because their potential broad effect on the gene expression. Moreover, TFs can function in different cell types of the brain. The same TF may affect different pathways in neurons and glia such as neurogenesis and inflammation, respectively. Identification of altered gene expression networks and the TFs involved opens the door for novel techniques to target cell-specific TF expression to restore homeostasis in diseased tissues.

CCAAT enhancer binding protein (C/EBP) β is a prolific TF that is involved in neurogenesis and inflammatory gene expression in the brain(Cortes-Canteli *et al*, 2011; Pulido-Salgado *et al*, 2015). Futhermore, C/EBPβ-mediated gene regulation has been implicated in Alzheimer's disease, amyotrophic lateral sclerosis, multiple sclerosis, Down's syndrome and HAND(Fields *et al*, 2011; Fields and Ghorpade, 2012; Figueroa-Romero *et al*, 2012; Liu *et al*, 2013; Pulido-Salgado *et al*, 2015; Ramberg *et al*, 2011). We previously reported that C/EBPβ expression is increased in brains of HIVE donors and HIV-relevant stimuli induce C/EBPβ expression in astroglia (Fields *et al*, 2011). We also showed that C/EBPβ contributes to the expression of 60% of a selected panel of interleukin (IL)-1β-induced astroglial inflammatory genes(Fields and Ghorpade, 2012). Other studies have shown that C/EBPβ is regulated in a cell-specific manner to alter neurogenesis, axonal injury, inflammation and differentiation depending on the cell type(Pulido-Salgado *et al*, 2015). Despite these findings, the specific cell types in which C/EBPβ is functioning in these different neurodegenerative diseases is unknown.

In this study we extended previous studies to characterize the cellular expression of C/EBPβ in the brains of HAND donors. We observed strong C/EBPβ signal in neurons of control and HIV+/HAND- brains, but HAND donors presented reduced C/EBPβ signal in neurons, and increased C/EBPβ signal in astroglia. These analyses suggest that HIV-relevant stimuli may have opposite effects on astroglial and neuronal C/EBPβ expression. These alterations in cellular C/EBPβ expression may underlie neurodegeneration and neuroinflammation in HAND patients.

Methods

Study population

For the present study, we evaluated brain tissues from a total of 33 HIV+ donors (**Table 1**) from the National NeuroAIDS Tissue Consortium (NNTC) (Institutional Review Board [IRB] #080323). All studies adhered to the ethical guidelines of the National Institutes of Health and the University of California, San Diego. These cases had neuromedical and neuropsychological examinations within a median of 12 months before death. Subjects were excluded if they had a history of CNS opportunistic infections or non-HIV-related developmental, neurologic, psychiatric, or metabolic conditions that might affect CNS functioning (e.g., loss of consciousness exceeding 30 minutes, psychosis, etc). HAND diagnoses were determined from a comprehensive neuropsychological test battery administered according to standardized protocols (Woods *et al*, 2004).

Neuromedical and neuropsychological evaluation

Participants underwent a comprehensive neuromedical evaluation that included assessment of medical history, structured medical and neurological examinations, and the collection of blood, cerebrospinal fluid, and urine samples, as previously described (Heaton *et al*, 2010; Woods *et al*, 2004). Clinical data (plasma viral load [VL], postmortem interval, CD4 count, global, learning and motor deficit scores [GDS, LDS, and MDS]) were collected for the HAND donor cohorts.

Neuropsychological evaluation was performed, and HAND diagnoses were determined via a comprehensive neuropsychological test battery, which was constructed to maximize sensitivity to neurocognitive deficits associated with HIV infection [see (Woods *et al*, 2004) for a list of tests]. Raw tests scores were transformed into demographically adjusted T-scores, including adjustments for age, education, gender and race. These demographically adjusted T-scores were converted to clinical ratings to determine presence and degree of neurocognitive impairment on seven neurocognitive domains, as previously described (Woods et al., 2004). As part of the neuropsychological battery, participants also completed self-report questionnaires of everyday functioning (i.e., Lawton and Brody Activities of Daily Living questionnaire; (Lawton and Brody, 1969), and/or Patient's Assessment of Own Functioning; PAOFI; (Chelune and Baer, 1986; Chelune, 1986). Participant's performance on the neuropsychological test battery and their responses to the everyday functioning questionnaires were utilized to assign HAND diagnoses following established criteria (Antinori *et al*, 2007), i.e., ANI, MND, and HAD.

ImmunoBlot

Frontal cortex tissues from human brains were homogenized in lysis buffer (1.0 mmol/L HEPES (Gibco, cat. no. 15630-080), 5.0 mmol/L benzamidine, 2.0 mmol/L 2-mercaptoethanol (Gibco, cat. no. 21985), 3.0 mmol/L EDTA (Omni pur, cat. no. 4005), 0.5 mmol/L magnesium sulfate, 0.05% sodium azide; final pH 8.8). In brief, as previously described (Fields *et al*, 2013), tissues from human brain samples (0.1 g) were homogenized by sonication for 15 seconds in 0.7 ml of lysis buffer containing phosphatase and protease inhibitor cocktails (Calbiochem, cat. no. 524624 and 539131). Samples were precleared by

centrifugation at 2000 × g for 5 min at room temperature. The supernatant was collected as representing the whole lysate.

After determination of the protein content of all samples by bicinchoninic acid assay (Thermo Fisher Scientific, cat. no. 23225) and denaturation in lamellae sample buffer, samples were loaded (20 µg total protein/lane) on 4–12% Bis-Tris gels (Invitrogen, cat. no. WG1402BX10) and electrophoresed in 5% HEPES running buffer and transferred onto PVDF membrane with iBlot transfer stacks (Invitrogen, cat. no. IB24001) using NuPage transfer buffer (ThermoFisher Scientific, cat. no NP0006). The membranes were blocked in 5% BSA in phosphate-buffered saline-tween 20 (PBST) for 1 h. Membranes were incubated overnight at 4 °C with primary antibody. Following visualization, blots were stripped and probed with a mouse monoclonal antibody against b-actin (ACTB; Sigma Aldrich, cat. no. A5441) diluted 1:2000 in blocking buffer as a loading control. All blots were then washed in PBST, and then incubated with species-specific IgG conjugated to HRP (American Qualex, cat. no. A102P5) diluted 1:5000 in PBST and visualized with SuperSignal West Femto Maximum Sensitivity Substrate (ThermoFisher Scientific, cat. no. 34096). Images were obtained, and semi-quantitative analysis was performed with the VersaDoc gel imaging system and Quantity One software (Bio-Rad).

Immunohistochemistry and double immunofluorescence

Free-floating 40 µm thick vibratome sections of human brains were washed with phosphate buffered saline (PBS) 3 times, pre-treated for 20 min in 3% H_2O_2, and blocked with 2.5% horse serum (Vector Laboratories, cat. no. S-2012) for 1 h at room temperature. Sections were incubated at 4 °C overnight with the primary antibody, C/EBPb (Santa Cruz Biotechnology; C-150) diluted in blocking buffer. Sections were then incubated in secondary antibody, Immpress HRP Anti-rabbit IgG (Vector, cat. no. MP-7401) for 30 min, followed by peroxidase (HRP) substrate made with DAB Peroxidase (HRP) Substrate Kit as per manufacturer's instructions (Vector, cat. no. SK-4800). Control experiments consisted of incubation with secondary antibody only. Tissues were mounted on Superfrost plus slides (Fisherbrand, cat. no. 12-550-15) and coverslipped with cytoseal (Richard Allen Scientific, cat. no. 8310-16). Immunostained sections were imaged with a digital Olympus microscope to identify C/EBPb immunoreactivity.

Double immunolabelling studies were performed as previously described(Spencer *et al*, 2009) to determine the cellular localization of C/EBPb. For this purpose, vibratome sections of human brains were immunostained with antibodies against C/EBPb with GFAP (Sigma Aldrich, cat. no. G3893), MAP2 (Santa Cruz Biotechnologies, cat# sc-32791), and IBA-1. Sections were then reacted with fluorescent secondary antibodies, goat anti mouse IgG 488 (Invitrogen, cat. no. A11011) and goat anti rabbit IgG 568 (Invitrogen, cat. no. A11036). Sections were mounted on superfrost plus slides and cover-slipped with vectasheild (Vector, cat. no. 1000). Sections were imaged with a Zeiss 63X (N.A. 1.4) objective on an Axiovert 35 microscope (Zeiss) with an attached MRC1024 laser scanning confocal microscope system (BioRad, Hercules, CA). An examiner blinded to sample identification analyzed all immunostaining. The precent colocalization was determined using Image J software with the SQASSH plug-in, as previously described.

In vitro studies of human astrocytes

This study was approved by the University of California San Diego Human Research Protections Program. Astroglia and neurons were isolated from fetal human brain tissue from elective terminated pregnancy between 12 and 16 weeks of gestation, acquired from Advanced Bioscience Resources. Donors gave written informed consent for research-use of the cells and tissue. Tissue was fragmented and mechanically dissociated using a scalpel and washed 3 times with HBSS holding media (Gibco, cat. no.14175-095) with 1 mM Glutamax (Gibco, cat. no. 35050-061), 20 µg/mL Gentamicin (Gibco, cat. no. 15710-064) and 5 mM HEPES (Gibco, cat. no. 15630-080). The tissue was homogenized with the addition of 15 mL of 0.25% trypsin EDTA (Gibco, cat. no. 25200-056) for 5 min in a 37 °C incubator. After 5 min, 1 mL of a trypsin inhibitor (Roche, cat. no. 10109) and 24 mL of DMEM media (Gibco, cat. no. 11960-044) with human serum (Corning, cat. no. 35-060-cl) was added. The mixture was then centrifuged for 5 min at 4 °C to pellet the cells. Supernatant was removed and discarded, and the cells were resuspended in 5 ml of DMEM media and strained with a 70 µM strainer (Falcon, cat. no. 352350). The cell suspension was underlaid with 7 ml of a solution of filtered 8% BSA in PBS and cells were centrifuged at 1 x 10^4 rpm at 4 °C for 10 min. The supernatant was removed, and the cells were resuspended in DMEM media with human serum for astroglia or Neurobasal media (Gibco, cat. no. 21103-049) for neurons containing 2% B27 supplement (Gibco, cat. no. 17504044), 1 mM Glutamax, and 20 µg/ml Gentamicin. Astroglia were plated at a density of 1 x 10^7/T75 flask and cultured as adherent monolayers. Neurons were plated on coverslips coated with poly-ornithine (Sigma Aldrich, cat. no. P4957) at a density of 2 x 10^5 cells/well and cultured as adherent monolayers. After 1 week, the astroglia DMEM media with human serum was replaced with DMEM media with 10% fetal bovine serum (Gibco, cat. no. 16000044) and 1% penicillin/ streptomycin (Corning, cat. no. 30-001-CI-1). Every 3 days, a half media exchange was performed on each cell type.

Transfection of astroglia with pC/EBPb

Astrocytes were split into 12 well plates at 500,000 cells/well on the day prior to transfection. Astrocytes were transfected using Lipofectamine 3000 (Thermo Fischer Scientific, cat. no. L3000075). Lipofectamine 3000 and an empty lentiviral expression plasmid (p) as a control or pC/EBPb (OriGene Technologies, Rockville, MD; CAT. SC319561) (1ug) in p3000 were diluted separately in Opti-Mem Media and then mixed together at a 1:1 ratio and left to incubate for 15 minutes at room temperature. After 15 minutes, the p-lipid complexes were added to the cells. Three days after transfection, RNA was isolated from astroglia.

RNA isolation and TaqMan® human inflammation array and real-time reverse transcription polymerase chain reaction (RT^2PCR)

Astroglia were split into 12 well plates at 5 x 10^5 cells/well for RNA isolation. Three days after transfection, media were removed and the cells were washed once with PBS. RNA was extracted with RNeasy plus mini kit (Qiagen, cat. no. 74136) according to manufacturer's instructions and analyzed for purity and concentration with a spectrophotometer. RNA was reverse transcribed into cDNA with a high capacity cDNA Reverse Transcription Kit (Life technologies, cat. no. 4358813) as per manufacturer's instructions. Taqman gene expression assays were performed using the StepOnePlus sequence-detection system (Life Technologies), using primers specific to DNM1L (Taqman, cat. no. hs00174131), IRAK1 (Taqman, cat. no. hs001155570), BCL11B (Taqman, cat. no. hs01102259), PINK1 (Taqman, cat. no. hs00260868), and ActB (Applied Biosystems, cat. no.1612290). A master mix was made using 5 µl of 2x Fast advanced master mix (Thermofisher Scientific, cat. no. 4444557), 0.5 µl of 20X primers, and 2 µl of water per reaction well. To each well of a microamp fast optical plate (Applied Biosystems, cat. no. 4346907), 8 µl of master mix and 2 µl of cDNA was added (The reactions were carried out at 48 °C for 30 min and 95 °C for 10 min, followed by 40 cycles of 95 °C for 15 s and 60 °C for 1 min). Samples were analyzed in duplicate. Fold changes were calculated using the comparative C_T method.

Antibodies

The following antibodies were used in immunoblot, immunohistochemistry, or both: C/EBPβ (Santa Cruz Biotechnology Inc.; catalog #sc-150), GFAP (Cell Signaling Technology; catalog #3670), NeuN (Abcam; catalog #104225), Iba-1 and β-actin (ACTB; Sigma-Aldrich; catalog #A2228).

Statistical analysis

All the analyses of images were conducted on coded samples blinded to the examiner. After the results were obtained, the code was broken and data were analyzed with Prizm software. Comparisons among groups were performed with one-way ANOVA with posthoc Fisher test and unpaired Student's T test where appropriate. All results were expressed as mean ±SEM. The differences were considered to be significant if p values were <0.05.

RNA library preparation

RNA sequencing libraries were generated using the Illumina TruSeq Stranded Total RNA Library Prep Gold with TruSeq Unique Dual Indexes (Illumina, San Diego, CA). Samples were processed following manufacturer's instructions, starting with 200 nanograms (ng) of RNA and modifying RNA shear time to five minutes. Resulting libraries were multiplexed and sequenced with 75 basepair (bp) single reads (SR75) to a depth of approximately 25 million reads per sample on an Illumina HiSeq 4000. Samples were demuxltiplexed using bcl2fastq v2.20 Conversion Software (Illumina, San Diego, CA).

Gene expression analysis

Total RNA was isolated from 50 mg of postmortem brain tissues from Broddmann Area 46 using the Qiagen RNeasy Lipid Tissue Kit per manufacturer instructions (Qiagen; cat# 74804). The mRNA libraries

were generated by the UC San Diego Institute for Genomic Medicine. RNA-seq data (75 bp single end reads with coverage of 20 million) was obtained from RNA extracted from the frontal cortex of MND and HIV+ cognitive normal subjects (CNHIV+). The quality of the raw FASTQ files were assessed using FASTQC v0.11.8. Adapters and low-quality reads were trimmed using a kmer approach as implemented in BBDuk v38.62. Transcripts were quantified using quasi-mapping mode of Salmon v0.14.1 (Patro *et al*, 2017) and summarized to gene counts for downstream analysis using the *tximport* v1.10.0 (Soneson *et al*, 2015) package. Genes were retained in the analysis if they achieved counts per million (cpm) > 1 in at least half of the brain samples sample. Effective library sizes were estimated by TMM scale-normalization prior to analysis to estimate observational weights (Law *et al*, 2014; Robinson and Oshlack, 2010). Surrogate variables representing latent noise were estimated using *sva* v package (JT *et al*, 2019). For the log-transformed expression data with precision weights, per-gene linear regression models were fit to account for the effects of cognitive impairment status after adjustment for unmodeled variation sources. Test for statistical significance was achieved by implementation of a Bayesian strategy of Lönnstedt and Speed as implemented in *R* package *limma* v3.38.3 (Ritchie *et al*, 2015). Significance was defined by using an adjusted p-value cut-off of 0.05 after multiple testing correction using a moderated t-static in limma.

To identify the underlying biological functions enriched in frontal cortex of MND relative to cognitive normal, Gene Set Enrichment Analysis (GSEA) was implemented which identifies the enrichment of functionally defined gene sets using a modified Kolmogorov-Smirnov statistic (Subramanian *et al*, 2005) and the Molecular Signature Database (MSigDb v6.0). Statistical significance after adjusting for multiple testing is defined at FDR < 0.05. Gene set-based permutation test of 1000 permutations was applied. Hypergeometric test was utilized to test the statistical significance of the enriched biological process and pathways identified for the unique differential expressed genes for each group (Yu *et al*, 2012). Overrepresentation enrichment analysis was conducted using the full set of detected genes as the reference gene set, corrected for multiple testing using the *Benjamini-Hochberg* procedure and FDR < 0.05 was considered significant. For the identified TF dysregulated in MND, differentially regulated targets were obtained using the experimentally validated TF binding profiles from the ChEA and ENCODE databases (Consortium, 2004; Lachmann *et al*, 2010). A database of gene expression in mature human astrocytes was created (Zhang *et al*, 2016) with threshold gene expression set at 1 FPKM per sample. The astrocyte marker genes were ranked according to the overall expression across all samples. Astrocyte marker genes were identified from C/EBPβ targets and hypergeometric test was used to analyze the functional pathway. All analysis were completed on R statistical software (v3.6.1) (Team, 2019)

Results

Clinical and neuropathological characteristics of HIV+ donors

A total of 33 NNTC autopsy cases were analyzed in order to assess relevant differences between postmortem brain samples from HIV patients. The brain tissues are characterized by age, sex, postmortem interval, education, VL and CD4+ cell count (**Table 1**). The average age did of each group did

not differ significantly and most of the cases were male. The postmortem interval (PMI) also did not differ significantly between the groups However, the average and standard deviation of PMI for the CN group was brought up by one case with a PMI of 200 hours. Education level also did not differ significantly between groups. The differences in CD4+ cell count between the groups were robust, with MND having the lowest average ($p= 0.102$ versus CN). Similarly, the differences in VL between groups approached significance with the MND group ($p=0.061$ versus CN) having the highest average. Data were analyzed using one-way ANOVA and Tukey's test for multiple comparisons.

C/EBPβ levels are increased in the astroglia and decreased in neurons in HAND cases

To determine the expression patterns of C/EBPβ in the frontal cortex of brains from control, HIV+/HAND-donors and HAND donors, we performed immunostaining for C/EBPβ in the frontal cortex. C/EBPβ signal was largely localized to pyramidal neurons, with a smaller proportion of the C/EBPβ signal in cells with glial morphology (black arrow), in brains from control and HIV+ donors with no cognitive impairment (**Fig. 1A**). In contrast, C/EBPβ signal is almost exclusively emanating from cells with glial morphology in brains from HAND donors (**Fig. 1A**). To determine the cellular expression of C/EBPβ in the brains of HAND patients, we double-immunolabeled the tissue sections for C/EBPβ (red) with astroglia (GFAP) or neurons (MAP2). C/EBPβ signal is faint in the nuclei of astroglia (GFAP+ cells) in brains from control and HIV+ cognitively normal cases, but the C/EBPβ signal in astroglia was robust in the brains from HAND cases (**Fig. 1B**). Quantification of colocalization of red and green signals showed that approximately 20% of C/EBPb (red) signal colocalized with GFAP (green) signal in CN brains compared to approximately 40% in HAND brains (**$p<0.05$; Fig. 1C**). C/EBPβ signal was strong in neurons (MAP2+) brains from HIV+ CN cases, but the C/EBPβ signal was less intense in neurons of HAND cases (**Fig. 1D**). Quantification of C/EBPβ+ neuronal cells revealed a 79 and 70% decrease in C/EBPβ colocalization with MAP2 in brains from HAND donors compared to brains from control and HIV+ donors, respectively ($p<0.05$; **Fig. 1E**).

We have previously reported that C/EBPβ levels are increased in the brains of HIV+ donors compared to control(Fields and Ghorpade, 2012). To confirm previous data, and determine C/EBPβ levels in this cohort, we isolated total RNA and protein from the brain tissues and analyzed for C/EBPβ mRNA and protein levels by RT^2PCR and immunoblot, respectively. C/EBPβ mRNA levels were increased 9-, 4- and 5-fold in brain tissues from ANI, MND and HAD donors, respectively ($p<0.05$; **Fig. 1F**). C/EBPβ protein detection by immunoblot revealed similar levels of the full C/EBPβ isoform in Normal and ANI tissues, but the bands corresponding to the full and LAP isoforms are more intense in the tissues from the MND and HAD brains (**Fig. 1G**). Quantification of the full and LAP bands showed similar C/EBPβ levels in Normal and ANI tissues, but the intensity of full and LAP bands was increased by 40% in tissues from MND and HAD brains ($p<0.01$; **Fig. 1H**).

Molecular signature of MND involves coordinated biological response and identifies transcriptional role of C/EBPβ

After filtering genes with low counts, adjusting for latent variables and multiple testing, a total of 1861 genes were differentially expressed in MND relative to HIV+ cognitively normal subjects (**Fig. 2A, Table S1**). The top upregulated genes are involved in immune response along with RNA editing which is vital for viral replication while the downregulated genes have role in synaptic maintenance along with novel pseudogenes. The subcellular distribution of differentially expressed genes was predominantly sequestered in cell junctions including synapses and associated with organelle membranes like the proteasome, mitochondria and the lipid-protein complex (**Fig. 2B**, **Table S2**). Functional analysis of the gene ontology revealed enrichment in protein processing, synaptic transmission, metabolic and immune processes (**Fig. 2C, Table S3**). Viral processes that allow for the survival of the virus including replication of genome and translation of viral mRNA by host ribosomes were also upregulated. Analysis of the disease-gene associations showed the differentially regulated genes were also implicated in other ailments with impaired cognition (**Table S4**). Specifically, Alzheimer's disease and tauopathy were enriched in the disease ontology (**Table S4**), suggesting potential convergence of the two pathologies (Canet *et al*, 2018).

TF analysis resulted in identification of twenty-six transcriptional regulators whose targets were enriched in MND and who were themselves differentially expressed (**Table S5**). C/EBPβ, which we have previously shown to be associated with HIVE, was upregulated and had 1308 targets that were differentially expressed in MND. Pathway analysis using REACOME and KEGG database identified the range of biological perturbations related to targets of C/EBPβ (**Fig. 2D, S1, Table S6**). In addition to regulating the expression of genes involved in immune and inflammatory response, targets of C/EBPβ are broadly involved in metabolism of protein and RNA, cell cycle, response to external stimuli and intracellular transport. While the genes corresponding to immune functions and autophagy were upregulated, downregulated gene set correspond to perturbed sphingolipid metabolism and ceramide production, consistent with observation in neural cells in HAND (Haughey *et al*, 2004).

To further identify the role of C/EBPβ in astrocytes based on analysis of the protein expression, astrocyte marker genes from the C/EBPβ targets were identified using a custom database of gene expression in mature human astrocytes (Zhang *et al*, 2016). From the targets of C/EBPβ a total of 1005 genes were astrocyte specific and almost all were upregulated (**Table S7**). In addition to the expected immune response, enriched pathways corresponded to metabolic function, signal transduction, RNA metabolism and autophagy (**Fig. 3, Table S8**). Subsequently, we find upregulation of KCNQ3, member of the potassium voltage-gated channel along with glutamate processing machinery including GLUL which converts neurotoxic glutamate to non-toxic glutamine, GRINA which is a subunit of glutamate ionotropic receptor and glutamate transporters (SLC1A2, SLC1A3). Taken together, these results show the comprehensive network of altered downstream effects of C/EBPβ in astrocytes.

Gene expression is altered in astroglia that over express C/EBPβ.

After transfecting astroglia with C/EBPβ, total RNA was extracted, transcribed into cDNA and relative levels of IRAK1, DNM1L, BCL11B and PINK1 mRNA were measured using rt^{2}PCR. C/EBPβ mRNA

overexpression was confirmed by measuring levels of C/EBPβ relative to ActB (**Fig. 4 A**). Overexpression of C/EBPβ also induced a significant increase in IRAK1 and DNM1L transcripts (**Fig. 4 B and C**). Increases in RNA expression for these markers suggest that increases in C/EBPβ in astroglia may increase immune response and affect mitochondrial dynamics. However, no significant difference was found between transfection and control for BCL11B, an immune regulator, and PINK1, a protector against mitochondrial dysfunction (**Fig. 4 D and E**).

Discussion

In the current study, we present RNAseq and transcriptomic analyses, neuropathological and biochemical data from FC brain tissues from a well characterized cohort of PWH. These findings support a role for the TF C/EBPb-mediated alterations in gene expression related to immune response, metabolic pathways, and autophagy in HAND. We report for the first time that C/EBPb expression is predominantly neuronal in CN brains. However, in HAND brains, C/EBPb is reduced in neurons and increased in astroglia. We found that C/EBPβ mRNA and protein levels were increased in a cohort of HAND brains compared to brains from CN HIV+ cases. Additionally, transcriptomic analyses confirmed increased C/EBPb mRNA and uncovered astrocyte marker genes amongst the differentially regulated C/EBPb targets. The role of C/EBPb in astroglia was further investigated by overexpressing C/EBPb in in vitro models for human astroglia. Multiple genes from the transcriptome of the HAND brains were overexpressed in the astroglia transfected with pC/EBPb. These findings are consistent with previous reports that show C/EBPβ activity and expression is altered in neurodegenerative disorders (Pulido-Salgado *et al*, 2015), and provides cell-type specific C/EBPβ expression patterns in HAND brains.

The transcriptome of HIV+ brains has been investigated in previous studies using gene arrays (Levine *et al*, 2013a; Levine *et al*, 2013b). However, to our knowledge this is the first time the transcriptome as defined by RNAseq technology has been reported in FC from CN and HAND brains. RNAseq offers a wide dynamic detection range and does not suffer from hybridization-based limitations associated with microarray such as background noise and saturation, or with probe set issues such as incorrect annotation and isoform coverage. Our findings are consistent with previous reports using gene arrays in which mitochondrial function and inflammation were found to be altered (Levine *et al*, 2013a; Levine *et al*, 2013b). Some of the highly upregulated genes including TRIM69, CTSB, B2M, UBE2L6, HLA and BTB3A3 have been previously reported to be associated with HAND (Siangphoe and Archer, 2015). The findngs presented here also support an overlap in neuropathogenic mechanisms between HAND and AD (**Table S4**), as has recently been the subject of many investigations (Achim *et al*, 2009; Fields *et al*, 2018; Mackiewicz *et al*, 2019; Sheppard *et al*, 2017). The current study extend these findings by identifying transcriptional deregulation in MND, specifically C/EBPb and linking its targets to marker genes in astroglia. This may be particularly important as astroglia have been recently implicated in metabolic complications of HAND and AD (Cisneros *et al*, 2018; Cisneros and Ghorpade, 2012; Jiang and Cadenas, 2014; Natarajaseenivasan *et al*, 2018; Swinton *et al*, 2019; Yin *et al*, 2016). Also consistent with the findings presented here, a recent study showed that YKL-40, a biomarker that reflects astroglial activation, is upregulated in cerebrospinal fluid from HAD cases and is associated with axonal injury (Hermansson

et al, 2019). These studies also illustrate a promising strategy to identify cell-specific alterations in gene expression that are identified in the transcriptome by combining traditional neuropathology and biochemical methods with novel RNAseq and systems biology techniques.

The altered transcripts indicating innate immune responses via the Toll-like receptors, Fc gamma receptors, TF NF-κB, cytokine type I interferons and MHC class I molecules are consistent with astrocytes response when exposed to HIV-1 (Daniels *et al*, 2017; El-Hage *et al*, 2005; Williams *et al*, 2009). Upregulation of ILF3 and IRAK1, key genes in innate antiviral immune response along with DKK3, an antagonist of Wnt signaling support the theory of astrocytes primed by cytokine signaling in aiding productive viral replication (Li *et al*, 2011). Alterations in glutamate uptake and potassium channels are associated with HIV-1 infection (Wang *et al*, 2003). Increased expression of calcium binding receptors (CALM1, CALM2) could be the result of excessive glutamate which can trigger increased levels of intracellular calcium levels in astrocytes. Nitrosative stress through increased nitric oxide production, known to be triggered by HIV protein Tat could mediate mitochondrial dysfunction facilitating in HIV mediated neuropathology (Liu *et al*, 2002b).

C/EBPβ is a TF involved in immune cell development, inflammatory responses, transcription from the HIV promoter, axonal injury, neurogenesis and autophagy regulation (Cortes-Canteli *et al*, 2011; Guo *et al*, 2013; Menard *et al*, 2002; Nadeau *et al*, 2005). Our current data are consistent with previous reports that show C/EBPβ is upregulated in immune-activated microglia and astroglia *in vitro*, in animal models of Alzheimer's and Huntington's diseases, and in the brains of donors with neurodegenerative disease (Fields *et al*, 2011; Fields and Ghorpade, 2012; Obrietan and Hoyt, 2004). Taken together with previous reports, our current results suggest that C/EBPβ is active in neurons in healthy brains, but neurons downregulate C/EBPβ in the context of HIV infection of the brain, while astrocytes increase C/EBPβ expression in HAND brains. This may reflect a sustained attempt by the host to mitigate neuronal loss and rid the brain of infection through astroglial immune responses. This is supported by reports that C/EBPβ controls transcription of genes regulating neurogenesis and responses to axonal injury in neurons and inflammation in astroglia (Cortes-Canteli *et al*, 2011; Fields *et al*, 2011; Liu *et al*, 2002a; Nadeau *et al*, 2005; Pulido-Salgado *et al*, 2015). Therapeutic targeting of C/EBPb transcription activity could potentially modulate inflammation while restoring neuronal activity directly.

The current findings are consistent with previous studies that showed altered autophagy and mitochondrial function in HAND brains (Alirezaei *et al*, 2008; Fields *et al*, 2015a; Fields *et al*, 2013; Fields *et al*, 2015c; Swinton *et al*, 2019). However, most previous studies have focused on the role of autophagy and mitochondria in neurons. The *in vitro* findings in this report support a role for C/EBPb autophagy and mitochondrial function in astroglia during HAND. Moreover, these findings corroborate several studies that have implicated C/EBPb in regulating autophagy (Guo *et al*, 2013; Ma *et al*, 2011). Although, overexpressing C/EBPb in astroglia may reveal some specific transcriptional activity of the TF, in an inflamed brain many other TFs are regulated (**Table S5**) and working in concert with C/EBPb to affect astroglial gene expression. This may explain why overexpressing C/EBPb had no effect on PINK1 and only marginal effect on BCL11b transcript levels in astroglia. Studies using mouse models for HIV-

induced neurotoxicity or other neurodegenerative diseases may offer a platform to better understand how C/EBPb contributes to neuropathogenesis.

Conclusions

These findings support a role for C/EBP dysregulation as a pathogenic mechanism underlying HAND. These data also suggest that cell-specific targeting of TFs may be used modulate neuronal and glial function. Future studies focusing on restoring neuronal C/EBPβ and modulating astroglial C/EBPβ function may facilitate proper neuronal function and reduce neuroinflammation in HAND patients. Future studies on C/EBPβ in neurodegenerative disorders should focus on cell type-specific pathways to design therapeutics targeting this prolific TF.

Abbreviations

HAND- HIV-associated neurocognitive disorders

FC-frontal cortex

C/EBP- CCAAT enhancer binding protein

TF-transcription Factor

MND-minor neurocognitive disorders

CN-cognitive normal

HIV-human immunodeficiency virus

PWH-people with HIV

ANI-asymptomatic neurocognitive Impairment

HAD-HIV associated Dementia

IL-interleukin

NNTC-National NeuroAIDS Tissue Consortium

VL-viral Load

PBST- phosphate-buffered saline-tween 20

PBS-phosphate buffered saline

P-plasmid

CNHIV+-HIV+ Cognitive normal subjects

Cpm-counts per million

Gsea-gene set enrichment analysis

PMI-post mortem interval

SLC1A2/3-subunit of glutamate ionotropic receptor and glutamate transporters

CALM1/2- Calcium binding receptors

pCON-Control plasmid

Declarations

Ethics approval and consent to participate: All studies adhered to the ethical guidelines of the National Institutes of Health and the University of California, San Diego. Postmortem human tissues were obtained from the National NeuroAIDS Tissue Consortium (NNTC) (Institutional Review Board [IRB] #080323).

Consent for publication: Not applicable

Availability of data and materials: All data and materials will be provided as available. Data generated from postmortem human samples will be deposited in the National NeuroAIDS Tissue Consortium database.

Competing Interests: The authors have no competing interests to report.

Funding This work was supported by National Institutes of Health (NIH) grants MH115819 (JAF) and NS105177 (JAF). This publication includes data generated at the UC San Diego IGM Genomics Center utilizing an Illumina NovaSeq 6000 that was purchased with funding from a National Institutes of Health SIG grant (#S10 OD026929). This publication was also made possible from NIH funding through the NIMH and National Institute on Neurological Diseases and Stroke by the following grants:

Manhattan HIV Brain Bank (MHBB): U24MH100931

Texas NeuroAIDS Research Center (TNRC): U24MH100930

National Neurological AIDS Bank (NNAB): U24MH100929

California NeuroAIDS Tissue Network (CNTN): U24MH100928

Data Coordinating Center (DCC): U24MH100925

Its contents are solely the responsibility of the authors and do not necessarily represent the official view of the NNTC or NIH. The funding bodies had no role in the design of the study or collection, analysis, and

interpretation of data or in writing the manuscript.

Author's Contributions: SC performed the transcriptomic analysis of the brain RNA and contributed to writing the manuscript. MS performed experiments using astroglia, the immunohistochemistry of human brain tissues and assisted editing the manuscript. RR contributed to writing the manuscript and the design of the transcriptomic analyses. JAF designed the project, planned the experiments, analyzed biochemical, molecular and neuropathological data, assisted with interpretation of the transcriptomic data, and drafted the paper.

Acknowledgements: Not applicable

References

Achim CL, Adame A, Dumaop W, Everall IP, Masliah E (2009). Increased accumulation of intraneuronal amyloid beta in HIV-infected patients. J Neuroimmune Pharmacol 4: 190-9.

Alirezaei M, Kiosses WB, Fox HS (2008). Decreased neuronal autophagy in HIV dementia: a mechanism of indirect neurotoxicity. Autophagy 4: 963-6.

Antinori A, Arendt G, Becker JT, Brew BJ, Byrd DA, Cherner M, Clifford DB, Cinque P, Epstein LG, Goodkin K, Gisslen M, Grant I, Heaton RK, Joseph J, Marder K, Marra CM, McArthur JC, Nunn M, Price RW, Pulliam L, Robertson KR, Sacktor N, Valcour V, Wojna VE (2007). Updated research nosology for HIV-associated neurocognitive disorders. Neurology 69: 1789-99.

Bingham R, Ahmed N, Rangi P, Johnson M, Tyrer M, Green J (2011). HIV encephalitis despite suppressed viraemia: a case of compartmentalized viral escape. Int J STD AIDS 22: 608-9.

Canet G, Dias C, Gabelle A, Simonin Y, Gosselet F, Marchi N, Makinson A, Tuaillon E, Van de Perre P, Givalois L, Salinas S (2018). HIV Neuroinfection and Alzheimer's Disease: Similarities and Potential Links? Frontiers in cellular neuroscience 12: 307-307.

Chelune GJ, Baer RA (1986). Developmental norms for the Wisconsin Card Sorting test. J Clin Exp Neuropsychol 8: 219-28.

Chelune GJ, Heaton R.K., & Lehman, R. A. (1986). Neuropsychological and personality correlates of patients' complaints of disability.

Cisneros IE, Erdenizmenli M, Cunningham KA, Paessler S, Dineley KT (2018). Cocaine evokes a profile of oxidative stress and impacts innate antiviral response pathways in astrocytes. Neuropharmacology 135: 431-443.

Cisneros IE, Ghorpade A (2012). HIV-1, methamphetamine and astrocyte glutamate regulation: combined excitotoxic implications for neuro-AIDS. Curr HIV Res 10: 392-406.

Clifford DB, Ances BM (2013). HIV-associated neurocognitive disorder. Lancet Infect Dis 13: 976-86.

Consortium TEP (2004). The ENCODE (ENCyclopedia Of DNA Elements) Project. Science 306: 636.

Cortes-Canteli M, Aguilar-Morante D, Sanz-Sancristobal M, Megias D, Santos A, Perez-Castillo A (2011). Role of C/EBPbeta transcription factor in adult hippocampal neurogenesis. PLoS One 6: e24842.

Daniels BP, Jujjavarapu H, Durrant DM, Williams JL, Green RR, White JP, Lazear HM, Gale M, Jr., Diamond MS, Klein RS (2017). Regional astrocyte IFN signaling restricts pathogenesis during neurotropic viral infection. The Journal of Clinical Investigation 127: 843-856.

El-Hage N, Gurwell JA, Singh IN, Knapp PE, Nath A, Hauser KF (2005). Synergistic increases in intracellular Ca2+, and the release of MCP-1, RANTES, and IL-6 by astrocytes treated with opiates and HIV-1 Tat. Glia 50: 91-106.

Fields J, Dumaop W, Elueteri S, Campos S, Serger E, Trejo M, Kosberg K, Adame A, Spencer B, Rockenstein E, He JJ, Masliah E (2015a). HIV-1 Tat alters neuronal autophagy by modulating autophagosome fusion to the lysosome: implications for HIV-associated neurocognitive disorders. J Neurosci 35: 1921-38.

Fields J, Dumaop W, Rockenstein E, Mante M, Spencer B, Grant I, Ellis R, Letendre S, Patrick C, Adame A, Masliah E (2013). Age-dependent molecular alterations in the autophagy pathway in HIVE patients and in a gp120 tg mouse model: reversal with beclin-1 gene transfer. J Neurovirol 19: 89-101.

Fields J, Gardner-Mercer J, Borgmann K, Clark I, Ghorpade A (2011). CCAAT/enhancer binding protein beta expression is increased in the brain during HIV-1-infection and contributes to regulation of astrocyte tissue inhibitor of metalloproteinase-1. J Neurochem 118: 93-104.

Fields J, Ghorpade A (2012). C/EBPbeta regulates multiple IL-1beta-induced human astrocyte inflammatory genes. J Neuroinflammation 9: 177.

Fields JA, Dumaop W, Crews L, Adame A, Spencer B, Metcalf J, He J, Rockenstein E, Masliah E (2015b). Mechanisms of HIV-1 Tat neurotoxicity via CDK5 translocation and hyper-activation: role in HIV-associated neurocognitive disorders. Curr HIV Res 13: 43-54.

Fields JA, Serger E, Campos S, Divakaruni AS, Kim C, Smith K, Trejo M, Adame A, Spencer B, Rockenstein E, Murphy AN, Ellis RJ, Letendre S, Grant I, Masliah E (2015c). HIV alters neuronal mitochondrial fission/fusion in the brain during HIV-associated neurocognitive disorders. Neurobiol Dis.

Fields JA, Spencer B, Swinton M, Qvale EM, Marquine MJ, Alexeeva A, Gough S, Soontornniyomkij B, Valera E, Masliah E, Achim CL, Desplats P (2018). Alterations in brain TREM2 and Amyloid-beta levels are associated with neurocognitive impairment in HIV-infected persons on antiretroviral therapy. J Neurochem 147: 784-802.

Figueroa-Romero C, Hur J, Bender DE, Delaney CE, Cataldo MD, Smith AL, Yung R, Ruden DM, Callaghan BC, Feldman EL (2012). Identification of epigenetically altered genes in sporadic amyotrophic lateral sclerosis. PLoS One 7: e52672.

Guo L, Huang JX, Liu Y, Li X, Zhou SR, Qian SW, Liu Y, Zhu H, Huang HY, Dang YJ, Tang QQ (2013). Transactivation of Atg4b by C/EBPbeta promotes autophagy to facilitate adipogenesis. Mol Cell Biol 33: 3180-90.

Haughey NJ, Cutler RG, Tamara A, McArthur JC, Vargas DL, Pardo CA, Turchan J, Nath A, Mattson MP (2004). Perturbation of sphingolipid metabolism and ceramide production in HIV-dementia. Annals of Neurology 55: 257-267.

Heaton RK, Clifford DB, Franklin DR, Jr., Woods SP, Ake C, Vaida F, Ellis RJ, Letendre SL, Marcotte TD, Atkinson JH, Rivera-Mindt M, Vigil OR, Taylor MJ, Collier AC, Marra CM, Gelman BB, McArthur JC, Morgello S, Simpson DM, McCutchan JA, Abramson I, Gamst A, Fennema-Notestine C, Jernigan TL, Wong J, Grant I (2010). HIV-associated neurocognitive disorders persist in the era of potent antiretroviral therapy: CHARTER Study. Neurology 75: 2087-96.

Hermansson L, Yilmaz A, Axelsson M, Blennow K, Fuchs D, Hagberg L, Lycke J, Zetterberg H, Gisslen M (2019). Cerebrospinal fluid levels of glial marker YKL-40 strongly associated with axonal injury in HIV infection. J Neuroinflammation 16: 16.

Jiang T, Cadenas E (2014). Astrocytic metabolic and inflammatory changes as a function of age. Aging Cell 13: 1059-67.

JT L, WE J, HS P, EJ F, AE J, JD S, Y Z, LC T (2019). sva: Surrogate Variable Analysis. R Package 3.32.1.

Lachmann A, Xu H, Krishnan J, Berger SI, Mazloom AR, Ma'ayan A (2010). ChEA: transcription factor regulation inferred from integrating genome-wide ChIP-X experiments. Bioinformatics (Oxford, England) 26: 2438-2444.

Law CW, Chen Y, Shi W, Smyth GK (2014). voom: precision weights unlock linear model analysis tools for RNA-seq read counts. Genome Biology 15: R29.

Lawton MP, Brody EM (1969). Assessment of older people: self-maintaining and instrumental activities of daily living. Gerontologist 9: 179-86.

Levine AJ, Horvath S, Miller EN, Singer EJ, Shapshak P, Baldwin GC, Martinez-Maza O, Witt MD, Langfelder P (2013a). Transcriptome analysis of HIV-infected peripheral blood monocytes: gene transcripts and networks associated with neurocognitive functioning. J Neuroimmunol 265: 96-105.

Levine AJ, Miller JA, Shapshak P, Gelman B, Singer EJ, Hinkin CH, Commins D, Morgello S, Grant I, Horvath S (2013b). Systems analysis of human brain gene expression: mechanisms for HIV-associated neurocognitive impairment and common pathways with Alzheimer's disease. BMC Med Genomics 6: 4.

Li W, Henderson LJ, Major EO, Al-Harthi L (2011). IFN-γ Mediates Enhancement of HIV Replication in Astrocytes by Inducing an Antagonist of the β-Catenin Pathway (DKK1) in a STAT 3-Dependent Manner. The Journal of Immunology 186: 6771-6778.

Liu M, Hou X, Zhang P, Hao Y, Yang Y, Wu X, Zhu D, Guan Y (2013). Microarray gene expression profiling analysis combined with bioinformatics in multiple sclerosis. Mol Biol Rep 40: 3731-7.

Liu X, Jana M, Dasgupta S, Koka S, He J, Wood C, Pahan K (2002a). Human immunodeficiency virus type 1 (HIV-1) tat induces nitric-oxide synthase in human astroglia. J Biol Chem 277: 39312-9.

Liu X, Jana M, Dasgupta S, Koka S, He J, Wood C, Pahan K (2002b). Human immunodeficiency virus type 1 (HIV-1) tat induces nitric-oxide synthase in human astroglia. The Journal of biological chemistry 277: 39312-39319.

Ma D, Panda S, Lin JD (2011). Temporal orchestration of circadian autophagy rhythm by C/EBPbeta. EMBO J 30: 4642-51.

Mackiewicz MM, Overk C, Achim CL, Masliah E (2019). Pathogenesis of age-related HIV neurodegeneration. J Neurovirol.

Menard C, Hein P, Paquin A, Savelson A, Yang XM, Lederfein D, Barnabe-Heider F, Mir AA, Sterneck E, Peterson AC, Johnson PF, Vinson C, Miller FD (2002). An essential role for a MEK-C/EBP pathway during growth factor-regulated cortical neurogenesis. Neuron 36: 597-610.

Nadeau S, Hein P, Fernandes KJ, Peterson AC, Miller FD (2005). A transcriptional role for C/EBP beta in the neuronal response to axonal injury. Mol Cell Neurosci 29: 525-35.

Natarajaseenivasan K, Cotto B, Shanmughapriya S, Lombardi AA, Datta PK, Madesh M, Elrod JW, Khalili K,Langford D (2018). Astrocytic metabolic switch is a novel etiology for Cocaine and HIV-1 Tat-mediated neurotoxicity. Cell Death Dis 9: 415.

Nath A (2002). Human immunodeficiency virus (HIV) proteins in neuropathogenesis of HIV dementia. J Infect Dis 186 Suppl 2: S193-8.

Obrietan K, Hoyt KR (2004). CRE-mediated transcription is increased in Huntington's disease transgenic mice. J Neurosci 24: 791-6.

Patro R, Duggal G, Love MI, Irizarry RA, Kingsford C (2017). Salmon provides fast and bias-aware quantification of transcript expression. Nature Methods 14: 417.

Pulido-Salgado M, Vidal-Taboada JM, Saura J (2015). C/EBPbeta and C/EBPdelta transcription factors: Basic biology and roles in the CNS. Prog Neurobiol 132: 1-33.

Ramberg V, Tracy LM, Samuelsson M, Nilsson LN, Iverfeldt K (2011). The CCAAT/enhancer binding protein (C/EBP) delta is differently regulated by fibrillar and oligomeric forms of the Alzheimer amyloid-beta peptide. J Neuroinflammation 8: 34.

Ritchie ME, Phipson B, Wu D, Hu Y, Law CW, Shi W, Smyth GK (2015). limma powers differential expression analyses for RNA-sequencing and microarray studies. Nucleic Acids Research 43: e47-e47.

Robinson MD, Oshlack A (2010). A scaling normalization method for differential expression analysis of RNA-seq data. Genome biology 11: R25-R25.

Sheppard DP, Iudicello JE, Morgan EE, Kamat R, Clark LR, Avci G, Bondi MW, Woods SP, Group HIVNRP (2017). Accelerated and accentuated neurocognitive aging in HIV infection. J Neurovirol 23: 492-500.

Siangphoe U, Archer KJ (2015). Gene Expression in HIV-Associated Neurocognitive Disorders: A Meta-Analysis. JAIDS Journal of Acquired Immune Deficiency Syndromes 70: 479-488.

Soneson C, Love M, Robinson M (2015). Differential analyses for RNA-seq: transcript-level estimates improve gene-level inferences [version 1; referees: 2 approved]. F1000Research 4.

Spencer B, Potkar R, Trejo M, Rockenstein E, Patrick C, Gindi R, Adame A, Wyss-Coray T, Masliah E (2009). Beclin 1 gene transfer activates autophagy and ameliorates the neurodegenerative pathology in alpha-synuclein models of Parkinson's and Lewy body diseases. The Journal of neuroscience : the official journal of the Society for Neuroscience 29: 13578-88.

Subramanian A, Tamayo P, Mootha VK, Mukherjee S, Ebert BL, Gillette MA, Paulovich A, Pomeroy SL, Golub TR, Lander ES, Mesirov JP (2005). Gene set enrichment analysis: A knowledge-based approach for interpreting genome-wide expression profiles. Proceedings of the National Academy of Sciences of the United States of America 102: 15545-15550.

Swinton MK, Carson A, Telese F, Sanchez AB, Soontornniyomkij B, Rad L, Batki I, Quintanilla B, Perez-Santiago J, Achim CL, Letendre S, Ellis RJ, Grant I, Murphy AN, Fields JA (2019). Mitochondrial biogenesis is altered in HIV+ brains exposed to ART: Implications for therapeutic targeting of astroglia. Neurobiol Dis 130: 104502.

Team RC (2019). R : A Language and Environment for Statistical Computing. In: R Foundation for Statistical Computing: Vienna, Austria.

Tozzi V, Uccella, I., Larussa, D., Lorenzini, P., Bossolasco, S., Bongiovanni, M., Moretti, F., Zannoni, P., Vigo, B., Mazzarello, G., Artioli, S., Monforte, A., Cingolani, A., Cinque, P., Antinori, A. (2003). Characteristics and factors associated with HIV-1 related neurocognitive disorders during HAART era. In: 5th International Symposium of NeuroVirology, HIV Molecular and Clinical Neuroscience Workshop. Khalili K, (ed). Taylor and Francis, in J NeuroVirol: Baltimore, MD, pp 10.

Wang Z, Pekarskaya O, Bencheikh M, Chao W, Gelbard HA, Ghorpade A, Rothstein JD, Volsky DJ (2003).Reduced expression of glutamate transporter EAAT2 and impaired glutamate transport in human primary astrocytes exposed to HIV-1 or gp120. Virology 312: 60-73.

Williams R, Yao H, Dhillon NK, Buch SJ (2009). HIV-1 Tat Co-Operates with IFN-γ and TNF-α to Increase CXCL10 in Human Astrocytes. PLOS ONE 4: e5709.

Woods SP, Rippeth JD, Frol AB, Levy JK, Ryan E, Soukup VM, Hinkin CH, Lazzaretto D, Cherner M, Marcotte TD, Gelman BB, Morgello S, Singer EJ, Grant I, Heaton RK (2004). Interrater reliability of clinical ratings and neurocognitive diagnoses in HIV. J Clin Exp Neuropsychol 26: 759-78.

Yin F, Sancheti H, Patil I, Cadenas E (2016). Energy metabolism and inflammation in brain aging and Alzheimer's disease. Free Radic Biol Med 100: 108-122.

Yu G, Wang L-G, Han Y, He Q-Y (2012). clusterProfiler: an R Package for Comparing Biological Themes Among Gene Clusters. OMICS: A Journal of Integrative Biology 16: 284-287.

Zhang Y, Sloan Steven A, Clarke Laura E, Caneda C, Plaza Colton A, Blumenthal Paul D, Vogel H, Steinberg Gary K, Edwards Michael SB, Li G, Duncan John A, III, Cheshier Samuel H, Shuer Lawrence M, Chang Edward F, Grant Gerald A, Gephart Melanie GH, Barres Ben A (2016). Purification and Characterization of Progenitor and Mature Human Astrocytes Reveals Transcriptional and Functional Differences with Mouse. Neuron 89: 37-53.

Table

Table 1. Clinical characteristics of the 33 brain specimens.

	Cognitive Normal (n=10)	Asymptomatic Neurocognitive Impairment (n=10)	Minor Neurocognitive Dysfunction (n=10)	HIV-Associated Dementia (n=3)
Age	41.7 ± 8.1	41.7 ± 10.8	43.1 ± 6.7	40.7 ± 2.1
Sex (fm:m)	0:10	1:9	1:9	1:2
Postmortem Interval	33.3 ± 67.5	21.4 ± 28.4	15.5 ± 14.4	9.3 ± 3.01
Education	13.0 ± 2.3	12.22 ± 3.4	12.0 ± 3.46	16.0 ± 3.5
CD4	151.6 ± 151.2	68.7 ± 73.9	35.3 ± 55.4	98.0 ± 155.1
VL (log)	3.3 ± 1.6	3.9 ± 1.3	5.0 ± 0.8	4.4 ± 2.4

Supplementary File Legends

Table S1. Related to Figure 2. Full differential gene expression (DGE) between MND and HIV+ cognitively normal subjects (CN HIV+)

Table S2. Related to Figure 2. Enriched cellular components between MND and CNHIV+

Table S3. Related to Figure 2. Enriched biological processes between MND and CNHIV+

Table S4. Disease-gene associations for differentially regulated genes in MND compared to CNHIV+

Table S5. List of differentially regulated TFs along with targets also differentially expressed in MND compared to CNHIV+

Table S6. Related to Figure 2. All enriched pathways for C/EBPβ targets in MND compared to CNHIV+

Table S7. Related to Figure 3. List of astrocyte specific marker genes that are also C/EBPβ targets in MND compared to CNHIV+

Table S8. Related to Figure 3. All enriched pathways for C/EBPβ regulated astrocyte marker genes targets in MND compared to CNHIV+

Figure S1. KEGG pathways shows distinct mechanisms between the C/EBPβ up and downregulated gene sets

Bar plots show the distinct pathways between the upregulated and down regulated target genes of C/EBPβ. The pathways are sorted by p-value which is calculated using the Fischer's exact test.

Figures

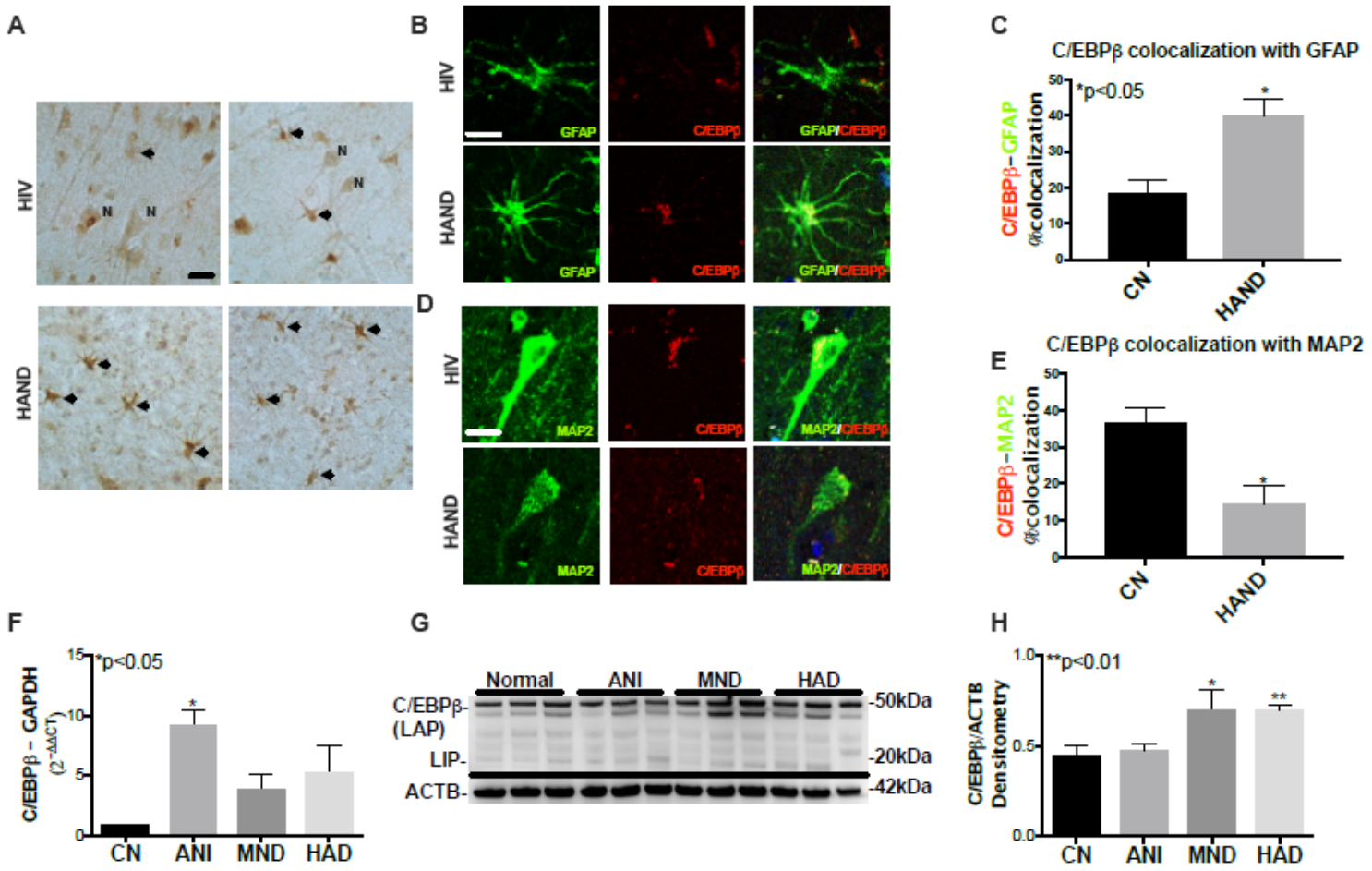

Figure 1

C/EBPβ levels are increased in the astroglia and decreased in neurons in HAND cases. (A) Vibratome sections of frontal cortex tissues from HIV CN and HAND cases w immunolabeled for C/EBPβ (n=4/group). Bar = 10□m (B) Vibratome sections from the frontal cortex from HIV CN and HAND cases double immunolabeled for GFAP (green) and C/EBPβ (red) (n=4/group). (C) The percent of C/EBPβ colocalizing with GFAP for CN versus HAND cases (n=4/group). (D) Double-immunolabeling was for MAP2 (green) and C/EBPβ (n=4/group). Bar = 10□m (E) Percent colocalization comparing CN and HAND cases. (F) RNA expression of C/EBPβ normalized to GAPDH plotted by neurocognitive status (n=33). (G) Western blot for C/EBPβ, (LAP), and LIP relative to ACTB using lysates of frontal cortex tissues (n=33). Band intensities for C/EBPβ plotted by neurocognitive status after normalization to ACTB (H). Statistical significance was determined by an unpaired t test when comparing two groups and by one-way ANOVA when comparing more than two groups (*p<0.05, ** p<0.01).

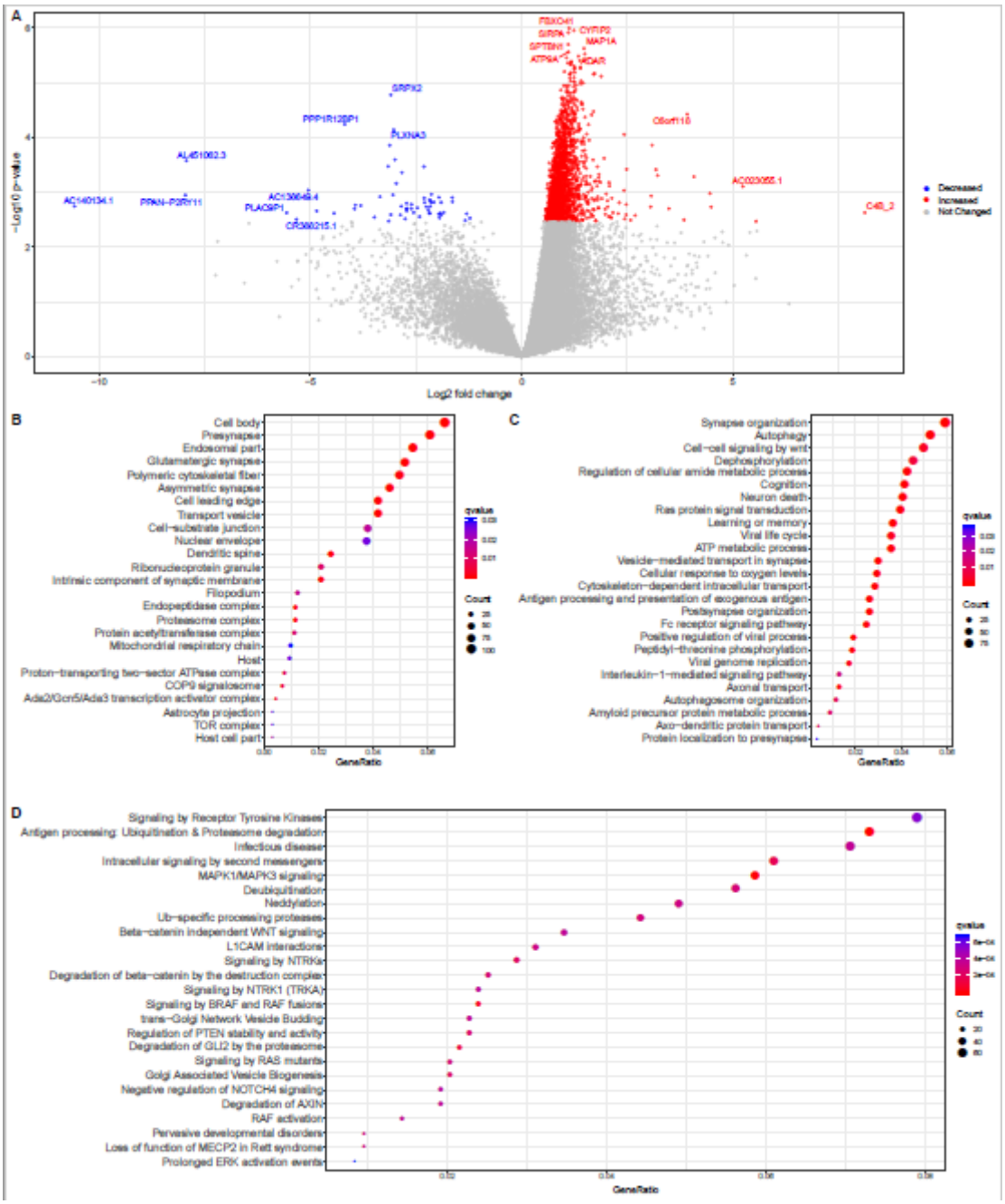

Figure 2

Global transcriptomic changes in HIV+ associated Minor Neurocognitive Disorders (MND) relative to controls. (A) Volcano plot of entire set of detected genes where each point represents the difference in expression (fold-change) between MND (n=10) and CN HIV+ (n=10) subjects plotted against the levels of statistical significance. Upregulated genes are represented in red, downregulated genes in blue and top genes in each spectrum are highlighted. (B-D) Gene ontology enrichment corresponding to cellular components (B) and biological process (C) across the differential genes in MND. Biological pathway analysis of differentially regulated C/EBPβ targets based on REACTOME database (D). The terms are arranged by number of differentially expressed genes associated to an enriched term and q-values where FDR < 0.05 was considered significant. For full list of gene ontology terms and pathways see Supplementary Tables S2, S3, S6.

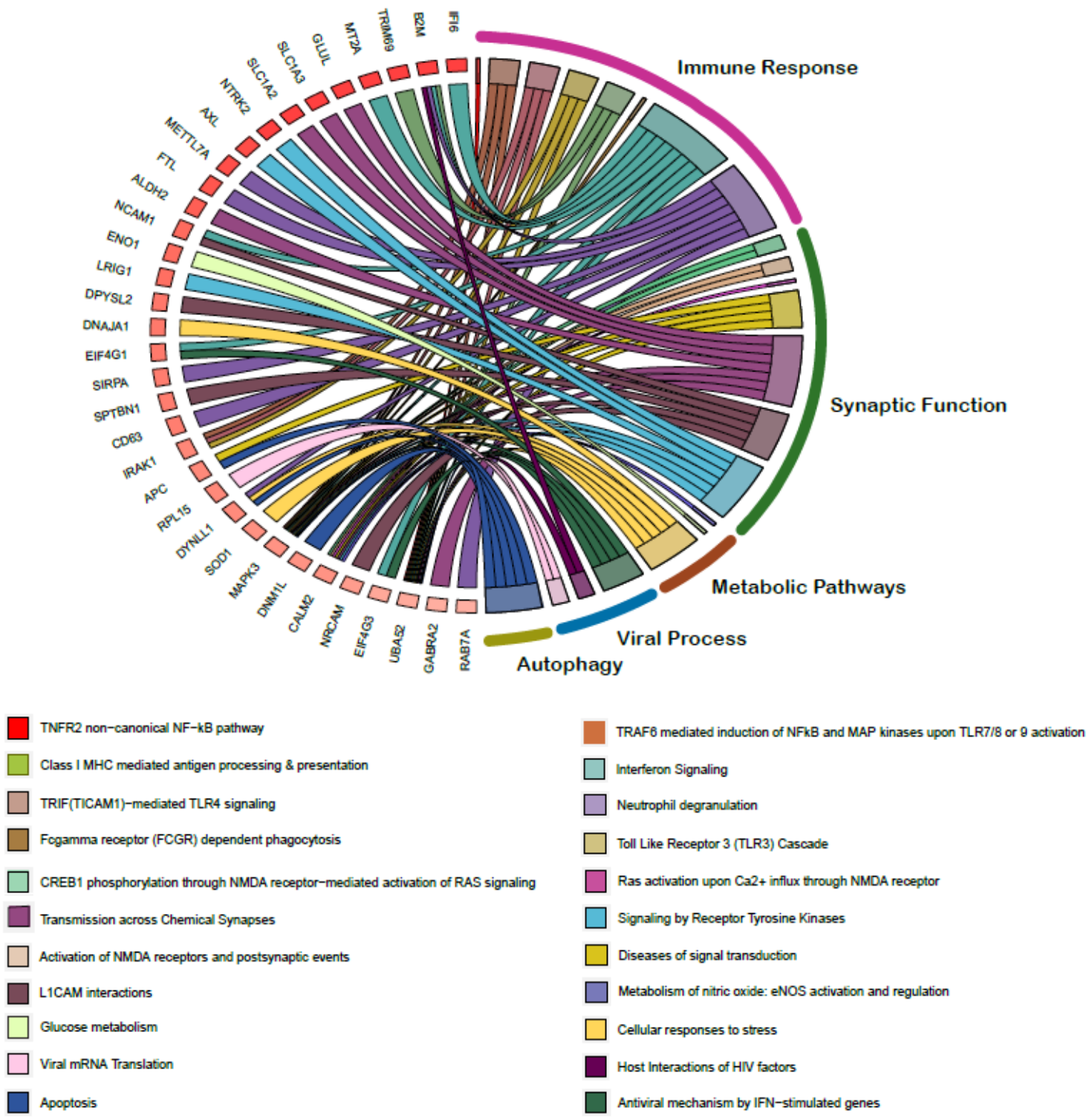

Figure 3

C/EBPβ targets in astrocytes are enriched for immune, metabolic and signal transduction pathways. Chord diagram showing the enriched REACTOME pathways for differentially regulated C/EBPβ targets that are also astrocyte marker genes. For chord diagrams, individual pathways are shown in the right and the enriched genes within the pathways are shown on the left. Squares following gene symbols represent the represents the difference in expression between MND and CNHIV+ subjects. Complete list of the

astrocyte marker genes that are also C/EBPβ targets is in Supplementary Table S7 and for enriched pathways corresponding to astrocyte marker genes, see Supplementary Table S8.

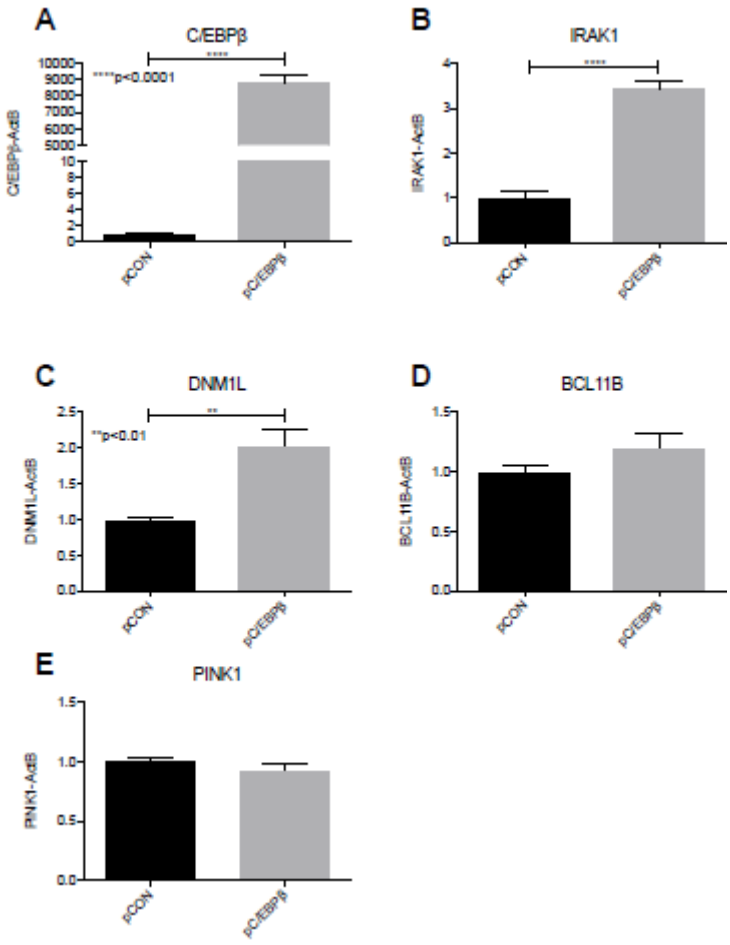

Figure 4

Gene expression is altered in astroglia that overexpress C/EBPβ. (A-E) Relative expression of mRNA for C/EBPβ (A), IRAK1 (B), DNM1L (C), BCL11B (D), and PINK1(E) in astroglia transfected with pControl (pCON) or pC/EBP. Statistical significance was determined by an unpaired t test (**p<0.01; ****p<0.0001). Data represent averages from at least three independent experiments.

Supplementary Files

This is a list of supplementary files associated with this preprint. Click to download.

- Supplementaryfigure1.pdf
- SupplementalMaterialsJNI.xlsx